

# Activity, selectivity, and long-term stability of different metal oxide supported gold catalysts for the preferential CO oxidation in H<sub>2</sub>-rich gas

Markus M. Schubert<sup>a,\*</sup>, Vojtech Plzak<sup>b,\*\*</sup>, Jürgen Garche<sup>b</sup> and R. Jürgen Behm<sup>a</sup>

<sup>a</sup> Abteilung Oberflächenchemie und Katalyse, Universität Ulm, D-89069 Ulm, Germany

E-mail: mmschubert@web.de

<sup>b</sup> Zentrum für Sonnenenergie- und Wasserstoff-Forschung (ZSW), Helmholtzstrasse 8, D-89081 Ulm, Germany

E-mail: vojtech.plzak@zsw-bw.de

Received 24 April 2001; accepted 13 July 2001

A comparative study of the catalytic performance and long-term stability of various metal oxide supported gold catalysts during preferential CO oxidation at 80 °C in a H<sub>2</sub>-containing atmosphere (PROX) reveals significant support effects. Compared to Au/ $\gamma$ -Al<sub>2</sub>O<sub>3</sub>, where the support is believed to behave neutrally in the reaction process, catalysts supported on reducible transition metal oxides, such as Fe<sub>2</sub>O<sub>3</sub>, CeO<sub>2</sub>, or TiO<sub>2</sub>, exhibit a CO oxidation activity of up to one magnitude higher at comparable gold particle sizes. The selectivity is also found to strongly depend on the employed metal oxide, amounting, *e.g.*, up to 75% for Au/Co<sub>3</sub>O<sub>4</sub> and down to 35% over Au/SnO<sub>2</sub>. The deactivation, which is observed for all samples with increasing time on stream, except for Au/ $\gamma$ -Al<sub>2</sub>O<sub>3</sub>, is related to the build-up of surface carbonate species. The long-term stability of the investigated catalysts in simulated methanol reformat depends crucially on the ability to form such by-products, with magnesia and Co<sub>3</sub>O<sub>4</sub> supported catalysts being most negatively affected. Overall, Au/CeO<sub>2</sub> and, in particular, Au/ $\alpha$ -Fe<sub>2</sub>O<sub>3</sub> represent the best compromise under the applied reaction conditions, especially due to the superior activity and the easily reversible deactivation of the latter catalyst.

**KEY WORDS:** selective CO oxidation; PROX; gold catalysts; preparation of Au/MeO<sub>x</sub>; support effects; long-term stability; deactivation; formation of carbonates; thermogravimetric measurements

## 1. Introduction

Oxide supported Au catalysts (Au/MeO<sub>x</sub>) have been shown to exhibit an outstanding activity already at low temperatures for several hydrogenation and oxidation reactions, in particular for CO oxidation (see, *e.g.* [1,2] and references therein). Consequently, gold catalysts, such as Au/MnO<sub>x</sub> [3] or Au/ $\alpha$ -Fe<sub>2</sub>O<sub>3</sub> [4,5], were also suggested as suitable candidates for the selective (preferential) CO oxidation in H<sub>2</sub>-rich gases (PROX) at low temperatures. The latter reaction is employed for the purification of feed gas streams for PEM (polymer electrolyte membrane) fuel cells produced *via* methanol steam reforming, the so-called reformat gas (*e.g.* [6]).

In previous comparative studies it was shown that the activity of Au/MeO<sub>x</sub> catalysts depends sensitively on the support material [7–11]. It was suggested that the high activity observed on Au/MeO<sub>x</sub> catalysts with easily reducible oxide supports results from cooperative effects of the support material, *i.e.*, its propensity for facile adsorption and storage of oxygen (*e.g.* [7,9,12–14]), which would result in a Mars–van Krevelen type reaction mechanism. So far, however, systematic, comparative studies on the influence of the support

material for different Au/MeO<sub>x</sub> catalysts and under identical conditions, exist only for the pure CO oxidation reaction (*e.g.* [8–11]). For the envisaged employment as PROX catalysts, not only the CO oxidation activity, but also the selectivity  $S$  ( $S = r^{\text{CO}}/[r^{\text{CO}} + r^{\text{H}_2}]$ , with  $r^{\text{X}}$  being the rates for CO and H<sub>2</sub> oxidation, respectively) and the long-term stability (approximately 5000 h lifetime are commonly assumed for mobile applications) are important key features.

Here we present results of a comparative study on the catalytic properties of various supported gold catalysts for the PROX reaction in simulated methanol reformat. Catalysts include Au/ $\alpha$ -Fe<sub>2</sub>O<sub>3</sub>, Au/TiO<sub>2</sub>, Au/CoO<sub>x</sub>, Au/NiO<sub>x</sub>, Au/Mg(OH)<sub>2</sub>, Au/CeO<sub>2</sub>, Au/SnO<sub>2</sub>, Au/MnO<sub>x</sub>, and Au/ $\gamma$ -Al<sub>2</sub>O<sub>3</sub>. The first two represent the most frequently investigated systems for pure CO oxidation (see, *e.g.* [9,15–19]); Au/CoO<sub>x</sub>, Au/NiO<sub>x</sub>, and Au/Mg(OH)<sub>2</sub> were proposed as highly active systems for the same reaction in preceding studies [2,20]. CeO<sub>2</sub> and SnO<sub>2</sub> are well established as active supports for CO oxidation over platinum metals (see, *e.g.* [21,22]), and therefore may also be expected to enhance the activity of attached gold particles. Au/MnO<sub>x</sub> was specifically suggested as a potential catalyst for the PROX reaction in H<sub>2</sub>-rich gas [3]. Finally, Au/ $\gamma$ -Al<sub>2</sub>O<sub>3</sub> is included as a reference material, since the latter support can be considered as inert at the low reaction temperature of 80 °C which is employed here. Specifically, it is not expected to enhance

\* Present address: BASF AG, Chemicals Research & Engineering (Catalysis Research), D-67056 Ludwigshafen, Germany.

\*\* To whom correspondence should be addressed.

the CO oxidation rate *via* support related oxygen storage or dissociation processes.

The Au/MeO<sub>x</sub> catalysts were prepared along individual, optimized routes (*i.e.*, most samples are representative of a larger group of similar Au/MeO<sub>x</sub> catalysts) and tested for their CO oxidation rate, selectivity, and long-term stability under identical conditions in simulated reformat. The catalytic measurements will demonstrate that the support material significantly affects both the activity as well as the selectivity of a catalyst, and also its long-term stability, with the Au/CeO<sub>2</sub>, and in particular the Au/Fe<sub>2</sub>O<sub>3</sub> systems representing the best compromise under the applied reaction conditions.

A brief description of the catalyst preparation and pretreatment procedures and the experimental set-up is given in section 2. Conversion measurements determining the activity and selectivity as a function of time (over 1000 min) are presented in section 3.1, followed by the gravimetric experiments on the deactivation process and a discussion of the combined deactivation results in section 3.2. Finally, the resulting conclusions are summarized.

## 2. Experimental

### 2.1. Preparation and pretreatment of catalysts

The Au/MeO<sub>x</sub> catalysts were generally prepared *via* standard methods, namely coprecipitation, deposition–precipitation or impregnation, which were optimized for the respective systems by varying the preparation parameters. The procedures are briefly summarized below. Further experimental parameters and characteristics such as precursor phases, pH values for precipitation, or precipitation temperature are given in table 1. The reproducibility of rates which was determined for samples prepared on identical routes was found to be  $\pm 30\%$  for Au/ $\alpha$ -Fe<sub>2</sub>O<sub>3</sub> and much better for most other samples.

#### 2.1.1. Coprecipitation (Au/ $\alpha$ -Fe<sub>2</sub>O<sub>3</sub>, Au/Ni<sub>2</sub>O<sub>3</sub>, Au/Mg(OH)<sub>2</sub>, and Au/MgO)

These catalysts (CP catalysts) were prepared in close accordance to the procedure described in [23]: aqueous solutions (each 1 M) of the respective metal nitrates (Fe(NO<sub>3</sub>)<sub>2</sub>·9H<sub>2</sub>O, Ni(NO<sub>3</sub>)<sub>2</sub>·6H<sub>2</sub>O, Mg(NO<sub>3</sub>)<sub>2</sub>·6H<sub>2</sub>O; all Fluka, p.a.) containing HAuCl<sub>4</sub>·3H<sub>2</sub>O (Merck, p.a.) and of Na<sub>2</sub>CO<sub>3</sub> (Fluka, p.a.) or NaOH (Merck, p.a.) for the Mg-containing supports, respectively, were added over 30 min to *ca.* 300 ml water at 60 °C and at a constant pH value. Stirring was continued for 30 min before the suspension was cooled to room temperature. The resulting precipitate was filtered and then washed and redispersed in water (*ca.* 40 °C) several times in order to eliminate chlorine and sodium residuals. Finally, the samples were dried in air at 80 °C and pulverized in an electric mill (only Au/ $\alpha$ -Fe<sub>2</sub>O<sub>3</sub>).

#### 2.1.2. Deposition–precipitation (Au/ $\alpha$ -Fe<sub>2</sub>O<sub>3</sub>, Au/CeO<sub>2</sub>, and Au/MnO<sub>2</sub>)

For Au/ $\alpha$ -Fe<sub>2</sub>O<sub>3</sub>, the support component was first precipitated in the same way as for the CP catalysts, but without addition of HAuCl<sub>4</sub>, similar to the route described in [24]. Subsequently, the Au-containing solution (0.15 M) was added, together with a Na<sub>2</sub>CO<sub>3</sub> buffer solution; within 5 min X-ray diffraction (XRD) and thermogravimetric (TGA) measurements showed that different from [24], none of the precursors for Au/ $\alpha$ -Fe<sub>2</sub>O<sub>3</sub> contained goethite. For Au/CeO<sub>2</sub>, the (Ce<sup>3+</sup>-free) support precursor was prepared by precipitation of CeO<sub>2</sub> from a 1 M aqueous solution of Ce(NH<sub>3</sub>)<sub>2</sub>(NO<sub>3</sub>)<sub>6</sub> (Fluka, p.a.) with 1 M Na<sub>2</sub>CO<sub>3</sub>. Before adding the Au-containing solution (see above), residual NH<sub>3</sub> was removed by repeated filtration, redispersion and heating to 80 °C. For the preparation of Au/MnO<sub>2</sub>, first NaMnO<sub>4</sub>·H<sub>2</sub>O (Fluka, purum) was reduced to MnO<sub>2</sub> by conc. HCl [25]. Subsequent treatment with 1 M HNO<sub>3</sub> yielded the H<sub>x</sub>MnO<sub>2-y</sub> precursor, which was impregnated with a solution of HAuCl<sub>4</sub> (0.1 M) at 60 °C and a pH value of 2 (buffered by LiOH).

Table 1  
Preparation/characterization of Au/MeO<sub>x</sub> catalysts.

Au on <sup>a</sup>	Meth.	Precursor	T <sub>precip</sub> (°C)	pH <sub>precip</sub>	Au <sup>b</sup> (at%)	BET <sup>a</sup> (m <sup>2</sup> /g)
$\alpha$ -Fe <sub>2</sub> O <sub>3</sub> (I)	DP	Fe <sub>5</sub> HO <sub>8</sub> ·4H <sub>2</sub> O + $\alpha$ -Fe <sub>2</sub> O <sub>3</sub>	80/60	7.8–8.2/8.3–8.1	0.94	63
$\alpha$ -Fe <sub>2</sub> O <sub>3</sub> (II)	CP	Fe <sub>5</sub> HO <sub>8</sub> ·4H <sub>2</sub> O	60	8.5	1.10	55
Ni <sub>2</sub> O <sub>3</sub> <sup>c</sup>	CP	NiCO <sub>3</sub> ·Ni(OH) <sub>2</sub>	60	8.5	1.72	67
Co <sub>3</sub> O <sub>4</sub>	IMP	Co <sub>3</sub> O <sub>4</sub>	60	7.1–7.8	0.44	49
Mg(OH) <sub>2</sub>	CP	Mg(OH) <sub>2</sub>	60	8.5	0.96	74
MgO	CP	Mg(OH) <sub>2</sub>	60	8.5	0.96	105
CeO <sub>2</sub>	DP	CeO <sub>2</sub>	60	6.5–7.0	2.24	105
MnO <sub>2</sub> <sup>d</sup>	DP	MnO <sub>1.97</sub> ·1.3H <sub>2</sub> O	60	1.9–2.2	0.92	134
TiO <sub>2</sub>	IMP	Degussa P25	60	5.0–5.5	1.77	56
$\gamma$ -Al <sub>2</sub> O <sub>3</sub>	IMP	Degussa 213	60	7.5–8.0	1.72	107
SnO <sub>2</sub>	IMP	SnO <sub>2</sub>	60	5.3–5.9	0.39	8

<sup>a</sup> After calcination at 400 °C (300 °C for Mg(OH)<sub>2</sub>).

<sup>b</sup> With reference to the oxide's metal.

<sup>c</sup> Ni<sub>2</sub>O<sub>3</sub> surface composition found by XPS; XRD indicates NiO for bulk.

<sup>d</sup> Containing 6.3 at% Li.

Table 2

Particle sizes after calcination, rate and selectivity (after 2 h) for the selective CO oxidation in idealized reformat (1 kPa CO, 1 kPa O<sub>2</sub>, 75 kPa H<sub>2</sub>, balance N<sub>2</sub>), and bulk phases, determined by XRD after 3 days in "more realistic" reformat (48.3 kPa H<sub>2</sub>, 13.8 kPa CO<sub>2</sub>, and 18.1 kPa H<sub>2</sub>O, balance N<sub>2</sub>) at 80 °C.

Au on <sup>a</sup>	$d_{\text{Ox}}$ <sup>a,b</sup> (nm)	$d_{\text{Au}}$ <sup>a,b,c,d</sup> (nm)	$D^e$ (%)	$r$ $\times 10^4 (\text{mol}_{\text{CO}}/(\text{g}_{\text{Au}} \text{ s}))$	$S$ (%)	Bulk transf. (XRD)
$\alpha\text{-Fe}_2\text{O}_3$ (I)	16.5	$2.3 \pm 0.8$	42	61	64	$\text{Fe}_3\text{O}_4 + \text{FeCO}_3$
$\alpha\text{-Fe}_2\text{O}_3$ (II)	15.4	$3.1 \pm 0.8$	33	46	63	$\text{Fe}_3\text{O}_4 + \text{FeCO}_3$
Ni <sub>2</sub> O <sub>3</sub>	9.0	$3.2 \pm 1.0$	30	20	56	–
Co <sub>3</sub> O <sub>4</sub>	17.0	$3.4 \pm 1.4$	24	22	75	–
Mg(OH) <sub>2</sub>	9.3–18.5	<4		13	67	–
MgO	5.3	$5.8 \pm 2.6$	14	3.8	64	–
CeO <sub>2</sub>	5.1	$2.2 \pm 0.6$	47	45	58	–
MnO <sub>2</sub>	7.4	$3.3 \pm 1.3$	26	1.4	~70	MnCO <sub>3</sub>
TiO <sub>2</sub>	21 <sup>f</sup>	$2.4 \pm 0.7$	42	33	48	–
TiO <sub>2</sub> <sup>g</sup>				51	53	–
$\gamma\text{-Al}_2\text{O}_3$	5.3–11.5	4.4	33 <sup>h</sup>	6.0	59	–
SnO <sub>2</sub>	38.4	$4.2 \pm 1.6$	22	14	32	–

<sup>a</sup> After calcination at 400 °C (300 °C for Mg(OH)<sub>2</sub>).

<sup>b</sup> XRD (via the Scherrer equation).

<sup>c</sup> Al<sub>2</sub>O<sub>3</sub>: Au(311).

<sup>d</sup> Average particle size, determined by TEM.

<sup>e</sup> Via number-averaged particle size.

<sup>f</sup> 92% anatase; 8% rutile ( $d = 26$  nm).

<sup>g</sup> After additional pretreatment in H<sub>2</sub> at 250 °C (20 Nml/min; 30 min).

<sup>h</sup> (Hemi-)spherical particles assumed [35].

All three samples were further stirred for 30 min, filtered, and dried, as described above.

### 2.1.3. Impregnation (Au/Co<sub>3</sub>O<sub>4</sub>, Au/TiO<sub>2</sub>, Au/ $\gamma$ -Al<sub>2</sub>O<sub>3</sub>, and Au/SnO<sub>2</sub>)

For Au/Co<sub>3</sub>O<sub>4</sub>, the oxidic support was prepared by thermal treatment of CoOOH in air at 400 °C. Previously, CoOOH was obtained by oxidation of Co(OH)<sub>2</sub> at 90 °C with air, according to [26]; Co(OH)<sub>2</sub> by precipitation from an aqueous solution of Co(NO<sub>3</sub>)<sub>2</sub>·6H<sub>2</sub>O (Fluka, p.a.) with NaOH. For the Au/SnO<sub>2</sub> catalyst, SnO<sub>2</sub> was prepared by oxidation of Sn (Heraeus, 99.999%) with concentrated HNO<sub>3</sub> and subsequent calcination of the resulting oxide at 910 °C (2 h). Finally, for Au/TiO<sub>2</sub> and Au/Al<sub>2</sub>O<sub>3</sub>, commercially available support materials (Degussa P25 and Degussa 213, respectively) were employed.

The pulverized oxides were suspended in 200 ml water (60 °C) and a solution of HAuCl<sub>4</sub> was added (within ca. 5 min), together with a Na<sub>2</sub>CO<sub>3</sub> buffer solution. The further processing of all samples (stirring, filtering and washing) was identical to that described above.

After preparation, the samples were stored in closed vessels at ambient conditions. All bright colored catalyst samples (e.g., Au/Al<sub>2</sub>O<sub>3</sub> or Au/TiO<sub>2</sub>) were stored in darkness in order to prevent light-induced reduction of the gold precursor, which, based on XRD measurements, leads to larger Au crystallites.

Prior to the experiments, the catalysts were calcined for 30 min in synthetic air for gravimetric measurements (110 Nml/min) or in 10 kPa O<sub>2</sub> in N<sub>2</sub> (20 Nml/min) at 400 °C for conversion measurements. This pretreatment, which reduces the Au to its metallic state, was found to produce the

most active and selective gold catalysts for PROX [27]. For the Au/Mg(OH)<sub>2</sub> sample a lower calcination temperature of 300 °C had to be used, since pretreatment at 400 °C yielded the corresponding Au/MgO sample. BET areas and the support phases after calcination as determined by XRD and X-ray photoelectron spectroscopy (XPS) are listed in table 1. The resulting average crystallite/particle sizes of the metal oxide support and of the gold particles after calcination, respectively, are included in table 2. It should be noted that no significant changes in the size distribution of the metal particles were observed on the time-scale of the thermogravimetric experiments in a simulated PROX atmosphere which are presented in the following.

Particle sizes were determined by TEM, except for Au/Mg(OH)<sub>2</sub> and Au/ $\gamma$ -Al<sub>2</sub>O<sub>3</sub>. For the latter they were calculated from XRD, using the Au(311) line. Since the gold particles on Au/Mg(OH)<sub>2</sub> were too small to be resolved by TEM or XRD, a dispersion of 50% was assumed for a rough estimate of the TOF (the latter may be considered as an upper limit).

### 2.2. Experimental arrangement

Activity measurements were carried out in a tubular quartz reactor (ID 4 mm) which contained approximately 100 mg of catalyst powder, fixed by quartz wool plugs. In order to guarantee differential conditions, the catalysts were diluted with  $\alpha$ -Al<sub>2</sub>O<sub>3</sub>. The gas mixture leaving the reactor tube was analyzed by a GC (Chrompack CP9001), equipped with wide-bore capillary columns (Poraplot U and Molsieve 5 Å; Chrompack) and thermal conductivity detectors. The mass-normalized rates (mol/(g<sub>Au</sub> s)) and the metal surface-

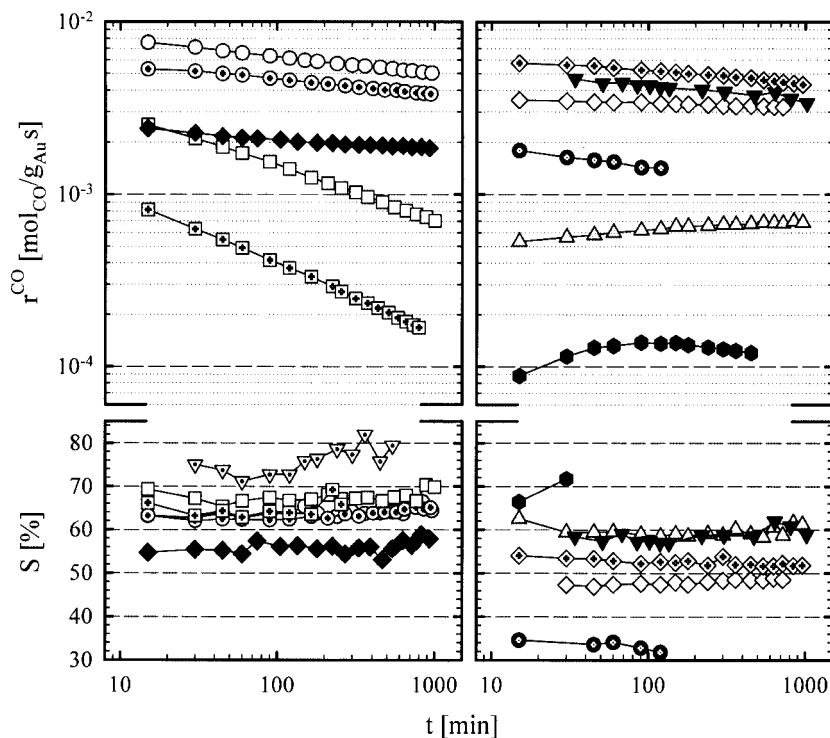


Figure 1. Rates (top) and selectivities (bottom) over different Au/MeO<sub>x</sub> catalysts during selective CO oxidation in idealized reformat as a function of time on stream (1 kPa CO, 75 kPa H<sub>2</sub>, balance nitrogen) and 1 kPa O<sub>2</sub> at 80 °C. Left side: Au/α-Fe<sub>2</sub>O<sub>3</sub> (I) (○), Au/α-Fe<sub>2</sub>O<sub>3</sub> (II) (⊙), Au/Co<sub>3</sub>O<sub>4</sub> (▽), Au/Ni<sub>2</sub>O<sub>3</sub> (◆), Au/Mg(OH)<sub>2</sub> (□), Au/MgO (▣); right side: Au/TiO<sub>2</sub> (◇) and after additional reductive pretreatment at 250 °C Au/TiO<sub>2</sub> (◊), Au/CeO<sub>2</sub> (▼), Au/SnO<sub>2</sub> (●), Au/γ-Al<sub>2</sub>O<sub>3</sub> (△), Au/MnO<sub>2</sub> (●).

normalized turnover frequencies (TOF (s<sup>-1</sup>)) were determined in an atmosphere containing 1 kPa CO, 75 kPa H<sub>2</sub>, and balance N<sub>2</sub> (denoted as “idealized reformat” in the following) at ambient pressures. 1 kPa O<sub>2</sub> was added for oxidation ( $\lambda = 2$ ). Preceding measurements showed that the data acquired in such a simplified atmosphere which enables a facile gas analysis by GC (and/or FTIR) are fairly well representative of the activity/selectivity in more realistic reformat gas feeds, which additionally contain large quantities of CO<sub>2</sub> and water [4,7,27].

The gravimetric long-term stability measurements were performed in a thermogravimetric micro balance apparatus (Shimadzu TA-50), equipped with a heated four-port valve which allowed for fast switching between the different gases. Since realistic reformat contains significant amounts of CO<sub>2</sub> and H<sub>2</sub>O, typically around 20–25% and 10–15%, respectively, a mixture of 48.3 kPa H<sub>2</sub>, 13.8 kPa CO<sub>2</sub> and 18.1 kPa water, balance N<sub>2</sub> was employed (110 Nml/min) for these experiments, which will be denoted as “more realistic” reformat in the following. (Unfortunately, CO could not be included due to security restrictions. The latter, however, is expected to exhibit only minor effects on the gravimetric results.)

The X-ray diffraction (XRD) measurements were performed on a Siemens D5000 spectrometer using the Cu K<sub>α</sub> line. For peak fitting, pseudo-Voigt functions were applied. Au and support crystallite sizes were determined by the Scherrer equation. Transmission electron microscopy (TEM) images were acquired on a Philips CM 20 micro-

scope. The gold dispersions were calculated via the number-averaged particle size, evaluating typically several hundred particles.

### 3. Results and discussion

#### 3.1. Comparison of the catalytic activity/selectivity

The activity/selectivity of the different Au/MeO<sub>x</sub> catalysts for the PROX reaction in idealized reformat and its evolution with time on stream (1000 min) is shown in figure 1. The CO oxidation rate ( $r^{\text{CO}}$ ) is displayed in the upper windows, the corresponding selectivity is shown below. The rates and selectivities, with the rates being normalized to the metal mass in the catalyst and the data taken after 2 h on stream, are also included in table 2. In order to rule out effects from a different metal dispersion in the different catalysts, due to varying particle sizes, the corresponding TOFs were determined as well, both at the beginning of the reaction, *i.e.*, after 15 min, and after 1000 min on stream. These are shown in figure 2.

Based on their TOFs, three different groups of catalysts can be distinguished. The group with the highest activity (*i.e.*, a TOF larger than 1 s<sup>-1</sup>) includes Au/α-Fe<sub>2</sub>O<sub>3</sub>, Au/Co<sub>3</sub>O<sub>4</sub>, Au/CeO<sub>2</sub>, Au/SnO<sub>2</sub>, Au/TiO<sub>2</sub>, and, having the lowest activity within that group, Au/Ni<sub>2</sub>O<sub>3</sub>. For Au/α-Fe<sub>2</sub>O<sub>3</sub>, which exhibits the highest activities, both preparation methods (CP and DP) yielded samples of similar particle sizes/particle size distributions and of comparable

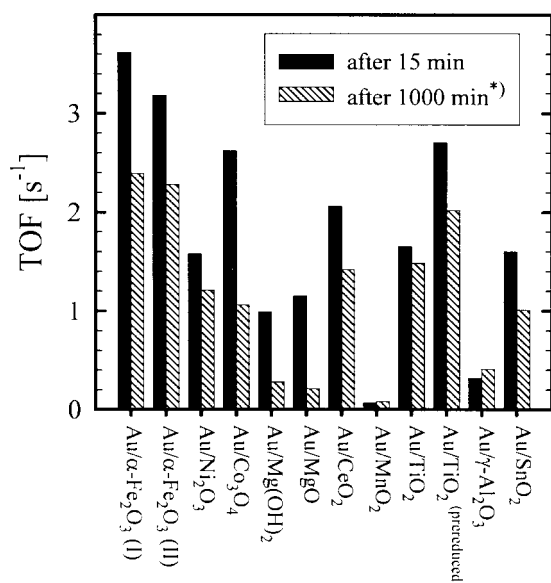


Figure 2. Turnover frequencies over different Au/MeO<sub>x</sub> catalysts in idealized reformat (1 kPa CO, 75 kPa H<sub>2</sub>, balance N<sub>2</sub>) and 1 kPa O<sub>2</sub> at 80 °C after 15 min and 1000 min on stream (\* rate after 15 min for Au/CeO<sub>2</sub> and rates after 1000 min for Au/TiO<sub>2</sub>, Au/SnO<sub>2</sub>, and Au/MnO<sub>2</sub>, respectively, were estimated by extrapolation of the data in figure 1).

activity and selectivity. Based on the initial activity, the Au/Co<sub>3</sub>O<sub>4</sub> catalyst is closest to Au/α-Fe<sub>2</sub>O<sub>3</sub>, but it deactivates much faster. On the other hand, Au/Ni<sub>2</sub>O<sub>3</sub>, which is initially less active, was much more stable against deactivation. As was expected from previous studies of CO oxidation on platinum metal catalysts, the SnO<sub>2</sub> and CeO<sub>2</sub> supports, which are known to be effective oxygen suppliers (*e.g.* [21,22,28,29]), yielded highly active samples as well. The Au/TiO<sub>2</sub> catalyst turned out to be especially active when additionally prereduced at 250 °C in flowing hydrogen (20 Nml/min, 30 min) after calcination, which was previously suggested as an effective pretreatment procedure for this catalyst [30,31]. The positive effect of the prereduction step is most likely related to an extensive formation of OH groups on the support surface, which is supported also by a distinct weight increase during reduction found in gravimetric experiments. This hydroxylation is apparently beneficial for the CO oxidation reaction. Other effects, such as a partial reduction of the support material may further contribute to the observed activity enhancement, however. The additional activation effect, however, diminishes with increasing time on stream so that the PROX rate slowly approaches the level of the unreduced sample.

The next group comprises Au/Mg(OH)<sub>2</sub> and Au/MgO. These two catalysts are clearly less active than the first group (initial TOFs around 1 s<sup>-1</sup>), but still significantly more active as compared to the Au/γ-Al<sub>2</sub>O<sub>3</sub> reference catalyst. The apparent difference between the Au/Mg(OH)<sub>2</sub> and Au/MgO catalysts in figure 1, indicated by the much lower mass-normalized activity of the latter one (about 30% of that on Au/Mg(OH)<sub>2</sub>), mainly results from the very different particles sizes of these two catalysts. While most of the Au/MeO<sub>x</sub> catalysts exhibit particle sizes around 3 nm,

these two systems deviate significantly with much larger (Au/MgO 5.8 nm average particle size) and much smaller (Au/Mg(OH)<sub>2</sub> amorphous in XRD and TEM) Au particle sizes. Based on TOFs, their activities are rather similar. The two MgO-based catalyst are also similar with respect to their rapid deactivation, which was so pronounced that at the end of the 1000 min runs their activity was significantly less (in TOFs) than that of the Au/γ-Al<sub>2</sub>O<sub>3</sub> reference sample. Possible effects underlying the rapid deactivation are discussed below.

The last group includes catalysts whose TOFs were clearly below 1 s<sup>-1</sup>. These are the Au/γ-Al<sub>2</sub>O<sub>3</sub> reference sample and Au/MnO<sub>2</sub>, which showed by far the lowest activity in this study. The latter was surprising, since MnO<sub>2</sub> is a further representative of a reducible transition metal oxide support, and therefore was expected to show a performance similar to the samples in the most active group. Several other preparation routes and different pretreatment procedures were tested, but no better Au/MnO<sub>x</sub> catalyst could be obtained. The measured rates, however, are in good agreement with the activity determined by Torres Sanchez *et al.* [3].

The sequence of relative activities for the PROX reaction found in our experiments agrees fairly well with the trend reported by Haruta *et al.* for the temperature of half conversion for pure CO oxidation, however, in absence of hydrogen [8,9]. The only exception is Au/Mg(OH)<sub>2</sub>, which was identified as one of the most active catalysts in the latter studies. A probable explanation for this apparent discrepancy are the extremely small gold particles of the Au/Mg(OH)<sub>2</sub> samples being used in those studies (around 1.2 nm [20]). Such small particles feature numerous undercoordinated edge and kink sites which were suggested to favor the direct oxygen dissociation on the metal [32]. This would increase the rate and TOF if the support is not or only barely involved in the oxygen supply for the CO oxidation reaction. Our results are also consistent with a study by Yuan *et al.* on a series of supported gold catalysts, prepared by impregnation of the corresponding hydroxides with phosphine-stabilized Au-complexes, where, *e.g.*, the CO oxidation started at much lower temperatures on samples like Fe(OH)<sub>3</sub>, Ni(OH)<sub>2</sub>, and Co(OH)<sub>2</sub> than on a Au/Al(OH)<sub>3</sub> sample (also hydrogen-free atmosphere [10]).

The observed activity differences were suggested to arise largely from the different abilities of the various support materials to supply the oxygen for the CO oxidation reaction [7,9,12,13]. The most active support materials, all of which are easily reducible metal oxides, are well known for their ability to adsorb and store oxygen and this way supply the oxygen required for the oxidation reaction *via* a second path, independent of direct (dissociative) oxygen adsorption on the Au particles. In a preceding study, this reaction path was exemplary demonstrated for the PROX reaction over a Au/α-Fe<sub>2</sub>O<sub>3</sub> catalyst [7]. In contrast, “inert” support materials such as MgO or, in particular, Al<sub>2</sub>O<sub>3</sub>, where this additional oxygen supply is not possible, are much lower in the activity scale. The variations within the latter group are possibly due to different Au particle shapes growing on the

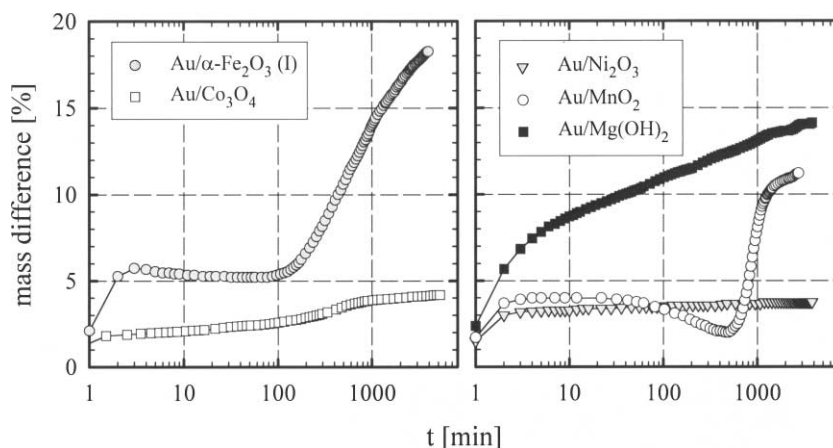


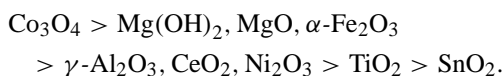
Figure 3. Mass evolution of selected Au/MeO<sub>x</sub> catalyst samples during reaction in “more realistic” reformat (48.3 kPa H<sub>2</sub>, 13.8 kPa CO<sub>2</sub>, and 18.1 kPa H<sub>2</sub>O, balance N<sub>2</sub>) at 80 °C, followed by gravimetric analysis.

different support materials (leading to an altered number of exposed, undercoordinated sites).

The good agreement of the activity and activity order, determined here for selective CO oxidation in idealized reformat, with that obtained for pure CO oxidation in a nitrogen background underlines that the presence of hydrogen has little effect on the CO oxidation reaction over such catalysts, similar to our findings in previous mechanistic studies of the PROX reaction over Au/α-Fe<sub>2</sub>O<sub>3</sub> [4,5].

If we now consider the selectivities of the different Au/MeO<sub>x</sub> catalysts in idealized reformat, distinct differences exist as well (figure 1, lower windows). The highest selectivities were observed for Au/α-Fe<sub>2</sub>O<sub>3</sub> (60–65%), Au/MgO, and Mg(OH)<sub>2</sub>, with 65–70%, respectively, and, in particular, for Au/Co<sub>3</sub>O<sub>4</sub> (75–80%). A second group, comprising Au/Ni<sub>2</sub>O<sub>3</sub>, Au/γ-Al<sub>2</sub>O<sub>3</sub>, and Au/CeO<sub>2</sub>, exhibits selectivities of roughly 55–60%. Over Au/TiO<sub>2</sub> (45–50%), and especially over Au/SnO<sub>2</sub> (30–35%), the selectivities are significantly smaller. A possible explanation may be an additional, direct catalysis of the competing H<sub>2</sub> + O<sub>2</sub> reaction on these support materials *via* a redox mechanism. This hypothesis is corroborated by the even lower selectivity (*ca.* 20%) observed for a Au/CeO<sub>2</sub> sample which additionally contained vanadia, which is well known for readily changing its oxidation state [27]. Nevertheless, a convincing and general explanation for the different selectivities does not yet exist. Note that the selectivity for Au/MnO<sub>2</sub> should be compared with reservation due to the exceptionally low reaction rate, causing large experimental errors of *ca.* ±15%.

Our results prove that the support material critically influences the selectivity. According to their (decreasing) selectivity in the PROX reaction under the present reaction conditions the different oxide support materials can be ordered in the following sequence:



Unfortunately, those Au/MeO<sub>x</sub> catalysts which exhibit the highest selectivity are also those that show the strongest de-

activation in figure 1, though a direct correlation between both phenomena is not obvious. The difference in deactivation is the subject of the next section, where we followed the long-term evolution of the composition of some selected catalyst samples by gravimetric measurements.

### 3.2. Long-term stability (gravimetric experiments)

In detailed, previous DRIFTS (diffuse reflectance FTIR) studies on the PROX reaction over Au/α-Fe<sub>2</sub>O<sub>3</sub> catalysts it was shown that increasing amounts of (surface) carbonate (CO<sub>3</sub><sup>2-</sup>) and carboxylate (CO<sub>2</sub><sup>-</sup>) species evolve with progressing time on stream, which were made responsible for the decreasing activity [27]. The gravimetric measurements in the “more realistic” reformat at 80 °C performed here, support these conclusions, as evidenced by the weight evolution of the Au/α-Fe<sub>2</sub>O<sub>3</sub> (I) sample with progressing time on stream (figure 3). After a first, rapid increase due to the adsorption of water and/or CO<sub>2</sub> on the surface, in a second stage the weight decreases slightly, which based on XRD measurements is attributed to the transformation of the α-Fe<sub>2</sub>O<sub>3</sub> support into Fe<sub>3</sub>O<sub>4</sub> (the latter represents the stable steady state of this support under PROX conditions). Subsequently, after *ca.* 2 h, a steady increase of the mass sets in again, which is now related to the progressing transformation of the support oxide into carbonate species. Correspondingly, XRD measurements performed after this treatment revealed strong reflexes of a siderite phase (FeCO<sub>3</sub>). Interestingly, the formation of the siderite phase was suppressed in the presence of small amounts of oxygen (0.3 kPa), as present in the PROX reaction, while DRIFTS experiments still showed the formation of surface carbonates. Hence, it is the latter species which are decisive for the deactivation during the PROX reaction/CO oxidation reaction. Consistently, for the Au/Ni<sub>2</sub>O<sub>3</sub> catalyst, which shows very little deactivation, only a very slow weight increase is recognized during time on stream, equivalent to a less pronounced tendency for carbonate formation. For the Au/α-Fe<sub>2</sub>O<sub>3</sub> sample the deactivation was shown to be easily reversible by flushing the catalyst bed with pure nitrogen

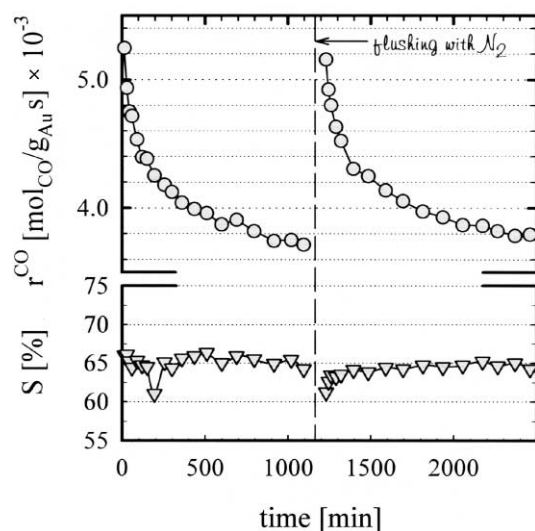


Figure 4. Activity (upper window) and selectivity (bottom) of Au/ $\alpha$ -Fe $_2$ O $_3$  (I) at 80 °C in idealized reformat before and after intermediate purging with 135 Nml/min of pure N $_2$  for 60 min after approximately 1200 min (dashed line). The lower initial activity of this run which was recorded several months after the measurement in figure 1 is mainly related to a slowly progressing coarsening of the Au particles during storage, as shown by XRD [27].

at the reaction temperature of 80 °C (figure 4; here, 1 h of flushing – 15 min, however, were also sufficient in other experiments). In parallel DRIFTS measurements it was shown that this procedure is accompanied by a significant decrease of previously accumulated surface carbonate species, corroborating the above proposed model [27].

A temporal evolution of the catalyst weight very similar to that of the Au/ $\alpha$ -Fe $_2$ O $_3$  catalyst is observed also for Au/MnO $_2$ . Following the initial H $_2$ O and CO $_2$  uptake, the subsequent weight loss indicates the reduction to Mn $_3$ O $_4$ , coinciding with an increase of activity in figure 1. Obviously, the latter phase supports the CO oxidation better than the initially prepared MnO $_2$  phase. In the following period, however, the oxide is rapidly transformed into MnCO $_3$  (strong increase of mass in figure 3), coinciding with the activity decrease occurring after *ca.* 200 min (figure 1). Note that for the latter sample the formation of bulk carbonates could not be suppressed by the addition of oxygen to the CO-free reformat, reflecting the higher thermodynamic stability of MnCO $_3$ . This fast formation of carbonates, which in severe cases even physically covered the Au particles, as evidenced by a strongly decreasing DRIFTS signal of CO $_{ad}$  adsorbed on the gold particles during reaction for some samples [27], is mainly held responsible for the surprisingly poor PROX performance of the Au/MnO $_2$  sample.

For the strongly deactivating Au/Mg(OH) $_2$  sample (the Au/MgO catalyst is not included in the figure, but exhibits a qualitatively similar behavior), we noticed a rapid increase of mass at the very beginning, followed by a further steady increase. This type of mass increase is predominantly attributed to the physisorption of water and CO $_2$ , similar to the assignment for the first stage on Au/ $\gamma$ -Fe $_2$ O $_3$ . Despite the known tendency of MgO to readily form carbonates in

a CO $_2$ -containing atmosphere (see, *e.g.* [33]), this interpretation seemed to be ruled out by subsequent XRD measurements, which showed no carbonate related reflexes. However, this apparent contradiction can be resolved if the carbonate is formed in a rather thin, compact layer only, which protects the bulk from further transformation and does not show up in XRD, but nevertheless impairs the CO oxidation reaction significantly. The formation of surface carbonates was also observed in recent DRIFTS measurements during CO oxidation on Au/MgO in idealized reformat, where large absorption bands in the region between 1200 and 1700 cm $^{-1}$  were rapidly growing [34]. An analogous explanation, formation of a thin surface layer of carbonates, is also assumed for Au/Co $_3$ O $_4$ , where only a small weight increase (compared to, *e.g.*, Au/ $\alpha$ -Fe $_2$ O $_3$ ) was observed in the “more realistic” reformat, contrasting the very strong deactivation (figure 1). Since MgO belongs most likely to the group of “inert” support materials which are not directly involved into the CO oxidation reaction, the strong negative impact of carbonate formation must be solely attributed to the physical covering of the Au particles by the produced carbonate layer.

As a consequence, the long-term stability of a Au/MeO $_x$  catalyst for the selective CO oxidation seems to be governed by its tendency to form surface carbonates under reaction conditions as well as by the stability of these layers. The formation of XRD detectable bulk carbonates by progressing transformation of the support oxide material is not required for the deactivation and is only a secondary effect. From this point of view, Au/TiO $_2$  and Au/ $\gamma$ -Al $_2$ O $_3$ , where surface carbonates form only very slowly – for the latter, virtually no bands between 1200 and 1700 cm $^{-1}$  were observed in DRIFTS measurements during selective CO oxidation in idealized reformat – would be the best candidates for long-term stable catalysts, if the activity and selectivity were considered only secondary.

For all catalysts investigated, the selectivity does not change with time on stream, in contrast to the CO oxidation activity. Consequently, under present reaction conditions the two competing reactions, CO oxidation and H $_2$  oxidation, are affected to a similar extent by the carbonate formation. This also supports a mechanistic interpretation according to which carbonate formation restricts the oxygen supply, which is equally required for both reactions. For catalysts supported on “inert” oxides, where oxygen supply from the support plays no role, one would correspondingly expect no or little carbonate induced deactivation, in accord with findings for Au/ $\gamma$ -Al $_2$ O $_3$ , except if carbonate formation occurs to an extent that the gold particles are physically blocked.

#### 4. Conclusions

The different Au/MeO $_x$  catalysts investigated exhibit significant differences in the CO oxidation activity in ideal reformat gas, with about one order of magnitude between the most active sample, Au/ $\alpha$ -Fe $_2$ O $_3$ , and the reference sample,

Au/ $\gamma$ -Al<sub>2</sub>O<sub>3</sub>. Since the gold particle sizes on the various samples are rather similar, particle size effects cannot be held responsible for these effects. Consequently, the differences are related to the different support materials, with easily reducible metal oxides, such as Fe<sub>2</sub>O<sub>3</sub>, CeO<sub>2</sub>, or TiO<sub>2</sub>, yielding the most active samples.

The PROX selectivity is strongly affected by the choice of the support material as well. It ranges between 35% for Au/SnO<sub>2</sub> and 75% for Au/Co<sub>3</sub>O<sub>4</sub> under the applied conditions. Consequently, the individual CO and H<sub>2</sub> oxidation reactions are affected to a different extent by the choice of the support oxide. The origin of those differences, however, is still unclear and requires further investigations.

The variations in long-term stability are related to the different tendencies of the various support oxides to form surface carbonates, which impairs both the CO and H<sub>2</sub> oxidation reactions, in a similar way. This is in agreement with a mechanistic interpretation according to which surface carbonate formation reduces the supply of oxygen required for both reactions. In particular the magnesia and Co<sub>3</sub>O<sub>4</sub> supported samples are strongly affected.

With respect to their suitability as long-term stable catalyst for the PROX reaction in (simulated) methanol reformate, Au/ $\alpha$ -Fe<sub>2</sub>O<sub>3</sub> represents the best compromise, due to its high activity in combination with a high selectivity. The still significant deactivation admittedly represents a drawback, since it requires loading the reactor with an initial excess of catalyst. However, even after 1000 min on stream Au/ $\alpha$ -Fe<sub>2</sub>O<sub>3</sub> is still the most active catalyst. Moreover, the complete reversibility of the deactivation over Au/ $\alpha$ -Fe<sub>2</sub>O<sub>3</sub> after a simple flushing of the catalyst bed with an inert gas suggests the use of regeneration cycles for practical applications. Au/CeO<sub>2</sub> comes closest to Au/ $\alpha$ -Fe<sub>2</sub>O<sub>3</sub> in its performance under the current reaction conditions and therefore represents an interesting alternative; especially, since it allows for a much simpler preparation of formed catalysts, e.g., pellets.

Finally, it should be noted that not only the proper choice of the support oxide is important in order to prepare a highly active gold catalyst. Recent results on various Au/CeO<sub>2</sub> and Au/SnO<sub>2</sub> catalysts suggest that the ratio between Au and oxide support particle size,  $d_{\text{Au}} : d_{\text{MeO}_x}$ , may affect the performance as well [27]. This is currently under investigation.

## Acknowledgement

We are grateful to F. Banhart (University Ulm) and the group around H. Bönemann (MPI für Kohlenforschung, Mülheim/Ruhr) for the TEM measurements. TiO<sub>2</sub> and Al<sub>2</sub>O<sub>3</sub> support materials (P25 and 213) were kindly provided by Degussa AG. We thank G. Feldmeyer for the XPS characterization of the Au/NiO<sub>x</sub> sample and A. Venugopal (University of Witwatersrand), M. Kinne, and Y.-F. Han (both University Ulm) for assistance during the activity measurements. Financial support for this work came from the state of Baden-Württemberg via the Zukunftsoffensive

Junge Generation. We are also grateful for a fellowship by the Deutsche Forschungsgemeinschaft for MMS, within the Graduiertenkolleg Molekulare Organisation und Dynamik an Grenz- und Oberflächen.

## References

- [1] G.C. Bond and D. Thompson, Catal. Rev. Sci. Eng. 41 (1999) 319.
- [2] M. Haruta, Catal. Surv. Jpn. 1 (1997) 61.
- [3] R.M. Torres Sanchez, A. Ueda, K. Tanaka and M. Haruta, J. Catal. 168 (1997) 125.
- [4] M.J. Kahlich, H.A. Gasteiger and R.J. Behm, J. Catal. 182 (1999) 430.
- [5] M.M. Schubert, M.J. Kahlich, H.A. Gasteiger and R.J. Behm, J. Power Sources 84 (1999) 175.
- [6] S. Kawatsu, J. Power Sources 71 (1998) 150.
- [7] M.M. Schubert, S. Hackenberg, A.C. van Veen, M. Muhler, V. Plzak and R.J. Behm, J. Catal. 197 (2001) 113.
- [8] M. Haruta, H. Kageyama, N. Kamijo, T. Kobayashi and F. Delannay, in: *Successful Design of Catalysts*, ed. T. Inui (Elsevier, Amsterdam, 1988) p. 33.
- [9] M. Haruta, S. Tsubota, T. Kobayashi, H. Kageyama, M.J. Genet and B. Delmon, J. Catal. 144 (1993) 175.
- [10] Y. Yuan, K. Asakura, H. Wan, K. Tsai and Y. Iwasawa, Chem. Lett. (1996) 755.
- [11] U. Rodmerck, P. Ignaszewski, M. Lucas and P. Claus, Chem. Ing. Tech. 71 (1999) 873.
- [12] M. Haruta, N. Yamada, T. Kobayashi and S. Iijima, J. Catal. 115 (1989) 301.
- [13] M.A.P. Dekkers, M.J. Lippits and B.E. Nieuwenhuys, Catal. Today 54 (1999) 381.
- [14] J.-D. Grunwaldt and A. Baiker, J. Phys. Chem. 103 (1999) 1002.
- [15] M.A. Bollinger and M.A. Vannice, Appl. Catal. B 8 (1996) 417.
- [16] J.-D. Grunwaldt, M. Maciejewski, O.S. Becker, P. Fabrizioli and A. Baiker, J. Catal. 186 (1999) 458.
- [17] A.I. Kozlov, A.P. Kozlova, H. Liu and Y. Iwasawa, Appl. Catal. 182 (1999) 9.
- [18] A.M. Visco, A. Donato, C. Milone and S. Galvagno, React. Kinet. Catal. Lett. 61 (1997) 219.
- [19] D. Horvath, L. Toth and L. Gucci, Catal. Lett. 67 (2000) 117.
- [20] D.A.H. Cunningham, W. Vogel, H. Kageyama, S. Tsubota and M. Haruta, J. Catal. 177 (1998) 1.
- [21] K. Grass and H.-G. Lintz, J. Catal. 172 (1997) 446.
- [22] C. Serre, F. Garin, G. Belot and G. Maire, J. Catal. 141 (1993) 9.
- [23] D. Andreeva, V. Idakiev, T. Tabakova, A. Andreev and R. Giovanoli, Appl. Catal. A 134 (1996) 275.
- [24] D. Andreeva, T. Tabakova, V. Idakiev, P. Christov and R. Giovanoli, Appl. Catal. A 169 (1998) 9.
- [25] F. Leroux, D. Guyomard and Y. Piffard, Solid State Ionics 80 (1995) 299.
- [26] M. Butel, L. Gautier and C. Delmas, Solid State Ionics 122 (1999) 271.
- [27] M.M. Schubert, Dissertation University of Ulm (2000).
- [28] C. Hardacre, R.M. Ormerod and R.M. Lambert, J. Phys. Chem. 98 (1994) 10901.
- [29] M.M. Schubert, M.J. Kahlich, G. Feldmeyer, M. Hüttner, S. Hackenberg, H.A. Gasteiger and R.J. Behm, Phys. Chem. Chem. Phys. 3 (2001) 1123.
- [30] N.W. Cant and N.J. Ossipoff, Catal. Today 36 (1997) 125.
- [31] S.D. Lin, M.A. Bollinger and M.A. Vannice, Catal. Lett. 17 (1993) 245.
- [32] M. Mavrikakis, P. Stoltze and J.K. Nørskov, Catal. Lett. 64 (2000) 101.
- [33] S.M. Ward, J. Braslaw and R.L. Gealer, Thermochim. Acta 64 (1983) 107.
- [34] S. Hackenberg, University of Ulm, personal communication.
- [35] M. Haruta, Catal. Today 36 (1997) 153.